JOURNAL OF MATERIALS SCIENCE 12 (1977) 919–926

Stress in an elastic wedge or notch loaded by a localized internal source

R. A. SACKS, J. E. ROBINSON
Solid State Science Division, Argonne National Laboratory, Argonne, Illinois, USA

A study is presented of the stress inside a two-dimensional elastic solid which has a boundary surface angle and which is loaded by an internal point source of expansion. An exact analytic solution for the stress is obtained, for general surface angle and source position, and evaluated numerically for several representative cases of wedges and notches. The singular behaviour given by the leading terms near the angle vertex is found to be highly localized, and there is little or no stress enhancement near the source. For many combinations of boundary angle and source location, however, a local region of significant enhancement occurs on that part of the surface nearest the source. Implications of these results are discussed, with particular reference to surface steps.

1. Introduction

Effects of irregularities in surface geometry on stress distributions in near-surface regions of solids play significant roles in diverse materials defect and failure phenomena. In this paper we analyse a two-dimensional prototype for the stresses due to a localized source applied near a surface angle or corner and present exact, general solutions for the stress distributions. Without attempting a broad survey, we first cite here some effects and phenomena that we have had in mind, and indicate circumstances in which exact solutions can be essential.

The importance of local stress-raising mechanisms to the description of brittle failure is well known [1], and it is generally accepted that fatigue cracks are initiated at some surface peculiarity [2]. A viable physical model for the recently reported sputtering of macroscopic chunks from the surfaces of metals under energetic neutron irradiation [3, 4] appears to require allowance for at least moderate stress enhancement near a neutron-induced collision cascade [5]. Since chemical attack is known to accelerate in regions of elevated stress*, a theory of the dynamics of corrosive chemisorption should take into account the influence of surface topography on local stress. Finally migration and interaction of crystal defects and impurities can be strongly affected by local stress patterns, and hence, be influenced by modification of these patterns by surface structures.

Most commonly, investigations of stress raising effects have employed one or both of two simplifications. Often the loading pattern chosen consists of a uniform stress applied over a substantial portion of the sample surface. Frequently, the stress analysis retains only the leading term of an expansion in the vicinity of a sharp feature or near-singularity of interest. Descriptions of stresses near crack tips in terms of conventional stress-intensity factors [6] exemplify this second type of approximation. However useful these two simplifications have proved, there are many problems of interest in which *neither* may be made with *a priori* assurance that an adequate description of the physical situation will survive. One example is a collision cascade, produced by energetic particle bombardment, located near the root of a surface step. The transient thermal stresses associated with the cascade obviously differ from uniform surface loading and, when knowledge of the total stress near the cascade is required, an expansion valid for the region asymptotically close to the step root can be quite unreliable. Similarly, in growth by diffu-

*For example, dislocations are commonly decorated by chemical etching.

sion of a precipitate in an alloy, one may be interested more in the stress field close to the boundary of the precipitate than in that at a near-by step root; here again a "leading term" approximation has uncertain validity. The complexities of a complete and realistic treatment of such situations are sufficiently great that it is very useful to study exactly soluble models which incorporate important physical features.

We study a two-dimensional wedge with an internal point source of expansion (Fig. 1), using linear elasticity theory. Since an extended source with circular symmetry is equivalent to an equal-strength point source at its centre, this model is adaptable to wedge-shaped surfaces with inclusions or voids or to three-dimensional wedges or wedge-shaped surface ridges which are loaded by cylindrical sources parallel to the wedge vertex (e.g. a long narrow collision cascade). In addition, since most of the effects should be localized near the wedge vertex, we may expect to gain at least qualitative understanding of the response of a surface step to a similar cylindrical stress source by a superposition of two wedges – one in which the internal angle α is less than π, and the other with $\alpha > \pi$. Our results may thus be compared with Marsh's [7] experimental finding of significant stress enhancement in the vicinity of the roots of a surface step subjected to the more conventional form of surface loading.

2. Analysis

In polar co-ordinates* it is easily shown that the stress components in an infinite medium surrounding a two-dimensional point source of expansion of strength δA at $\mathbf{r}_0 = (r_0, \theta_0)$ are

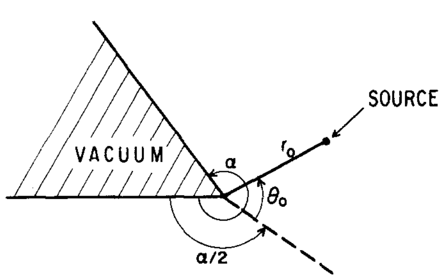

Figure 1 A two-dimensional wedge of total interior angle α is loaded by an internal point source of expansion. The source is located a distance r_0 from the wedge vertex and at an angle θ_0 from the wedge bisector.

$$\begin{aligned}
\sigma_{rr} &= (\mu\delta A/\pi)\,[-|\mathbf{r}-\mathbf{r}_0|^{-2} + 2r_0^2 \\
&\qquad \sin^2(\theta-\theta_0)\,|\mathbf{r}-\mathbf{r}_0|^{-4}] \\
\sigma_{\theta\theta} &= (\mu\delta A/\pi)\,[|\mathbf{r}-\mathbf{r}_0|^{-2} - 2r_0^2 \\
&\qquad \sin^2(\theta-\theta_0)\,|\mathbf{r}-\mathbf{r}_0|^{-4}] \\
\sigma_{r\theta} &= -2(\mu\delta A/\pi) r_0 \sin(\theta-\theta_0) \\
&\qquad [r - r_0\cos(\theta-\theta_0)]\,|\mathbf{r}-\mathbf{r}_0|^{-4},
\end{aligned} \tag{1}$$

where μ is the shear modulus for the material. Choosing units such that $\mu\delta A/\pi = 1$, the maximum shearing stress τ, given by

$$\tau = [\tfrac{1}{4}(\sigma_{rr} - \sigma_{\theta\theta})^2 + \sigma_{r\theta}^2]^{1/2}, \tag{2a}$$

reduces for the point source to

$$\tau = |\mathbf{r}-\mathbf{r}_0|^{-2}. \tag{2b}$$

In the interior of a wedge the stress components in these units are

$$\begin{aligned}
\sigma_{rr} &= -|\mathbf{r}-\mathbf{r}_0|^{-2} + 2r_0^2\sin^2(\theta-\theta_0)|\mathbf{r}-\mathbf{r}_0|^{-4} \\
&\qquad + [r^{-1}(\partial/\partial r) + r^{-2}(\partial^2/\partial\theta^2)]\,\chi \\
\sigma_{\theta\theta} &= |\mathbf{r}-\mathbf{r}_0|^{-2} - 2r_0^2\sin^2(\theta-\theta_0)|\mathbf{r}-\mathbf{r}_0|^{-4} + \\
&\qquad \partial^2\chi/\partial r^2 \\
\sigma_{r\theta} &= -2r_0\sin(\theta-\theta_0)\,[r - r_0\cos(\theta-\theta_0)] \\
&\qquad |\mathbf{r}-\mathbf{r}_0|^{-4} - (\partial/\partial r)(r^{-1}\partial\chi/\partial\theta)
\end{aligned} \tag{3}$$

where χ is the Airy function [9] satisfying the biharmonic equation

$$\nabla^4\chi = 0, \tag{4}$$

and we must choose the solution which causes the total stress on the boundary planes to vanish

$$\sigma_{r\theta} = \sigma_{\theta\theta} = 0 \quad \text{at } \theta = \pm\alpha/2. \tag{5}$$

Our method of solution is an extension of Sneddon's treatment of a symmetrically loaded wedge [10]. With the introduction of the Mellin transform

$$\bar{\chi}(S,\theta) = \int_0^\infty r^{S-1}\,\mathrm{d}r\,\chi(r,\theta), \tag{6}$$

the biharmonic equation reduces to

$$(S^2 + \partial^2/\partial\theta^2)[(S+2)^2 + \partial^2/\partial\theta^2]\,\bar{\chi}(S,\theta) = 0. \tag{7}$$

*See, for example [8] for definitions of stress and strain components and the statement of Hooke's law in plane polar co-ordinates.

The general solution to Equation 7 is

$$\bar{\chi}(S,\theta) = A(S)\sin(S\theta)+B(S)\cos(S\theta) + C(S)\sin[(S+2)\theta] + D(S)\cos[(S+2)\theta]. \quad (8)$$

Multiplying the last two of Equations 3 by r^{S+1}, setting $\theta = \pm\alpha/2$, integrating over r^*, and using Equation 5 yields four algebraic equations for the coefficients A, B, C, D. These are easily solved to find

$$\bar{\chi}(S,\theta) = (\pi r_0^S/S)\{\cot(S\theta)\cos[S(\theta-\theta_0)] + \sin(S\theta_0)g(S,\alpha,\theta)/G(S,\alpha) + \cos(S\theta_0)h(S,\alpha,\theta)/H(S,\alpha)\}, \quad (9)$$

where

$$-2 < \operatorname{Re} S < 0,$$

$$\begin{aligned} g(S,\alpha,\theta) &= \{(S+1)\cos(\alpha)+\cos[(S+1)\alpha]\} \sin(S\theta) - S\sin[(S+2)\theta], \\ h(S,\alpha,\theta) &= \{(S+1)\cos(\alpha)-\cos[(S+1)\alpha]\} \cos(S\theta) - S\cos[(S+2)\theta], \\ G(S,\alpha) &= (S+1)\sin(\alpha)-\sin[(S+1)\alpha], \\ H(S,\alpha) &= (S+1)\sin(\alpha)+\sin[(S+1)\alpha]. \end{aligned} \quad (10)$$

The stress is then found from Equations 3 and the Mellin inversion formula†

$$\chi(r,\theta) = (2\pi i)^{-1}\int_{C-i\infty}^{C+i\infty} r^{-S}\bar{\chi}(S,\theta)\,dS \qquad -2<C<0. \quad (11)$$

Before applying Equation 11, one technical difficulty must be resolved. If $\alpha > \pi$, G and H will generally have roots – and hence $\bar{\chi}$ will have poles – in the region $-2 < \operatorname{Re}(S) < 0$ (aside from the obvious pole at $S=-1$ which, it turns out, does not contribute to the stress). Different allowable choices of C will thus lead to different solutions for the stress; that is, the original boundary value problem is underdetermined‡. The additional boundary conditions necessary to specify the solution uniquely are supplied by the physical requirement that the components of the displacement,

$$\begin{aligned} U_r &= (2\pi)^{-1}\delta A\,[r - r_0\cos(\theta-\theta_0)]\,|\mathbf{r}-\mathbf{r}_0|^{-2} + \mu\delta A(2\pi^2 Ei)^{-2}\int_{C-i\infty}^{C+i\infty} dS\, r^{-S-1}(S+1)^{-1} \times [S+S(S+1)\nu - \partial^2/\partial\theta^2]\,\bar{\chi} \\ U_\theta &= (2\pi)^{-1}\delta A\, r_0\sin(\theta-\theta_0)|^{-2} - 2r_0^2 - \mu\delta A(2\pi^2 Ei)\int_{C-i\infty}^{C+i\infty} dS\, r^{-S-1}(S+1)^{-1} (S+2)^{-1} \times [2S^2+3S+2+\partial^2/\partial\theta^2 + \nu(S+1)(S+2)]\,\partial\bar{\chi}/\partial\theta \end{aligned} \quad (12)$$

(E is Young's modulus) must be finite everywhere. In particular, they must be finite as $r \to 0$ and as $r \to \infty$. This stipulation implies that the correct choice of contour is $C = -1$§.

On substituting Equations 9 and 10 into Equation 11, one can verify that for all values of C the integrand vanishes exponentially for $\operatorname{Im}(S) \to \pm\infty$, and the line integral converges. Accordingly, for $r > r_0$ the line of integration may be moved off to $C = \operatorname{Re}(S) \to +\infty$ and $\chi(r,\theta)$ is the sum of the contributions from poles to the right of $\operatorname{Re}(S) = -1$. Similarly, for $r < r_0$, $\chi(r,\theta)$ is the sum of the residues at poles to the left of $\operatorname{Re}(S) = -1$.

Substituting $\chi(r,\theta)$ so evaluated into Equations 3 gives

$$\begin{aligned} \sigma_{rr} &= \mp\pi r^{-2}\Big\{\sum' [(S\partial G/\partial S)^{-1}(r_0/r)^S \sin(S\theta_0)(\partial^2 g/\partial\theta^2 - Sg)]_{S=S_g} + \sum_{S_h}' (S\partial H/\partial S)^{-1}(r_0/r)^S \cos(S\theta_0)(\partial^2 h/\partial\theta^2 - Sh)]_{S=S_h} \\ \sigma_{\theta\theta} &= \mp\pi r^{-2}\Big\{\sum_{S_g}' [(\partial G/\partial S)^{-1}(r_0/r)^S \sin(S\theta_0)(S+1)g]_{S=S_g} + \sum_{S_h}' [(\partial H/\partial S)^{-1}(r_0/r)^S\Big\} \cos(S\theta_0)(S+1)h]_{S=S_h} \end{aligned} \quad (13)$$

*See [11] p. 309, for the Mellin transforms of the source terms.

†See [11] p. 307.

‡This indeterminacy may be thought of as reflecting the possibility of adding elastic multipoles at the origin and "at infinity" which satisfy the confitions of exerting no stress on the boundary planes. See [12].

§The "correct" choice is actually either $C=-1-\epsilon$ or $C=-1+\epsilon$ ($\epsilon \approx 0$), since $\bar{\chi}$ has a pole at $S=-1$. As this pole makes no contribution to the stress (although it does contribute to the displacement), the question of which choice is correct is not addressed in detail.

$$\sigma_{r\theta} = \mp \pi r^{-2} \left\{ \sum_{S_g}' [(S\partial G/\partial S)^{-1} (r_0/r)^S \sin(S\theta_0)(S+1)\partial g/\partial\theta]_{S=S_g} + \sum_{S_h}' [(S\partial H/\partial S)^{-1} (r_0/r)^S \cos(S\theta_0)(S+1)\partial h/\partial\theta]_{S=S_h} \right\}.$$

In Equations 13, S_g and S_h are the roots of G and H, respectively, the primed sums run over the roots $\mathrm{Re}(S_g, S_h) > -1$ for $r > r_0$ and $\mathrm{Re}(S_g, S_h) < -1$ for $r < r_0$, and the upper (lower) sign applies for $r > r_0 (r < r_0)$. Table I lists the first few roots for several values of α.

Several properties of the sums in Equations 13 are apparent. The roots S_g and S_h occur in complex conjugate pairs, so the sums are manifestly real. The roots $S_g = -2, -1, 0$ and $S_h = -1$ do not contribute, because the corresponding residues vanish. The dominant behaviour at both large and small r is determined by the roots lying closest to $\mathrm{Re}(S) = -1$, and, as the values in Table I indicate, these are always roots of H. Since the roots occur in pairs symmetric with respect to $S = -1$, we may write the leading behaviour at small r as $r^{-\beta}$ and at large r as $r^{\beta-2}$, where β varies monotonically from $-\infty$ when $\alpha = 0$, through 0 when $\alpha = \pi$, to $+\frac{1}{2}$ when $\alpha = 2\pi$. The square root singularity at $r = 0$ for $\alpha = 2\pi$ corresponds precisely to that found by Wigglesworth for notched planes [13, 14] and to the familiar result for the stress concentration near the tip of a sharp crack*. Note that α is 1/2 *only* for this flat slit limit, although it remains nearly 1/2 for $\alpha \gtrsim (3\pi/2)$, and, hence, it is clear that one should exercise some restraint in wholesale application of crack tip formulae. For $\alpha < \pi$, the stresses vanish at the origin. The effect of the surface angle on the stress persists to large distances. While the stress from a point source in an infinite medium falls off as r^{-2}, here the stress vanishes asymptotically more rapidly for $\alpha < \pi$ and more slowly for $\alpha > \pi$.

TABLE I The roots S_g and S_h of G and H (Equations 10). When a value for y is given, four roots are formed from the combinations $S = -1 + x \pm iy$. and $S = -1 - x \pm iy$. When y is not shown, only the two roots $S = -1 \pm x$ occur. The values $S_g = -2, -1, 0$ and $S_h = -1$ are roots of G and H for any α but are not shown since they do not contribute to the sums in Equations 13

α	x_g	y_g	x_h	y_h
$\pi/4$	9.6	3.4	5.4	2.7
	17.7	4.1	13.7	3.8
	25.8	4.6	21.7	4.4
$\pi/2$	4.8	1.5	2.7	1.1
	8.9	1.8	6.8	1.7
	12.9	2.1	10.9	2.0
$3\pi/4$	3.2	0.64	1.9	0.36
	5.9	0.90	4.6	0.79
	8.6	1.1	7.3	0.99
$5\pi/4$	1.3	–	0.67	–
	2.8	0.33	2.0	0.22
	4.4	0.46	3.6	0.40
$4\pi/3$	1.1	–	0.62	–
	2.6	0.35	1.8	0.25
	4.1	0.46	3.3	0.41
$3\pi/2$	0.91	–	0.54	–
	2.3	0.32	1.6	0.23
	3.6	0.42	3.0	0.37
$7\pi/4$	0.66	–	0.51	–
	2.0	0.16	1.4	0.011
	3.1	0.26	2.6	0.22

3. Numerical results

Numerical evaluation of the sums in equations 13 reveals that this "leading term" analysis is incomplete. Figs. 2 to 5 are contour plots for a few values of α of the maximum shearing stress τ, Equations 2a, and of a stress enhancement factor κ defined by

$$\kappa = \tau_{\text{total}}/\tau_{\text{applied}}. \tag{14}$$

The behaviour for both large and small r described in the last section is present: as $r \to 0$, both τ and κ vanish for $\alpha < \pi$ and diverge for $\alpha > \pi$; as $r \to \infty$, κ vanishes for $\alpha < \pi$ and increases for $\alpha > \pi$. However, as is clearly shown in the plots, this behaviour holds only for $(r/r_0) \gg 1$ (where τ is much too small to have significant effect) or for $(r/r_0) \ll 1$ (where the approximation of a sharp corner is most critical). In the immediate neighbourhood of the source, all wedges investigated have κ between 0.9 and 1.1. That is, the effects of the boundary are insignificant in the region of maximum stress. There is, however, an interesting feature on the wedge surface. For all values of θ_0 when $\alpha < \pi$, and for some values of θ_0 when $\alpha > \pi$, there is a localized region on the surface, near the point of closest approach to the source, where κ attains values between 1.8 and 2.1.

In general, the shapes of the contours for τ, as opposed to their spacing, exhibit only slight

*See [14] Chpt. 2.

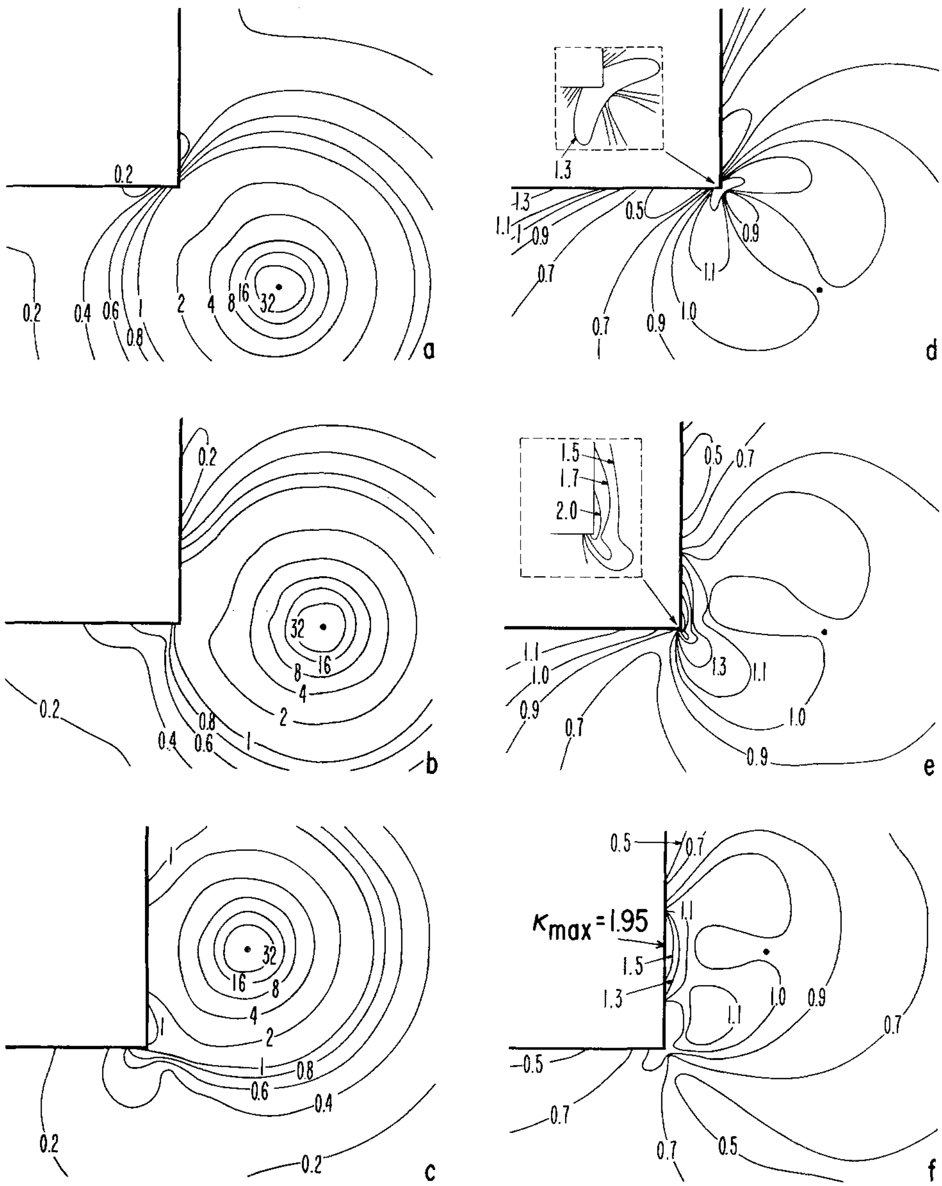

Figure 2 Contour plots of τ, Equation 2a, and κ, Equation 14. τ is measured in units of $(\mu\delta A/\pi r_0^2)$. Co-ordinates are defined in Fig. 1. Inserts, surrounded by dashed lines in the vacuum region, are expanded views of the neighbourhood of the angle vertex. τ (a) to (c); κ (d) to (f). $\alpha = (3\pi/2)$. θ_0: 0 in (a) and (d) $\pi/4$ in (b) and (e), and $\pi/2$ in (c) and (f). Note that $0.9 < \kappa < 1.0$ at the source, while (f) exhibits a local "hot spot" with $\kappa = 1.95$ on the surface.

distortions from the circular symmetry they would have in an infinite medium, save quite close to the boundary. Although appreciable structure does appear in the contour plots for κ, it should be noted that the changes in κ from one contour to the next are rather small.

4. Discussion

As discussed in Section 1, we expect stresses near the top and near the root of a macroscopic surface step to be approximated by those we have found for wedges with $\alpha < \pi$ and $\alpha > \pi$, respectively. The localized shielding of the applied stress we find near the origin for $\alpha < \pi$, and the localized divergence found for $\alpha > \pi$ are in agreement with Marsh's [8] findings of little or not stress near his step tops and of high stress near his step roots. Our result of little stress modification near the source is in accord with Marsh's stress contours since these show little stress concentration at

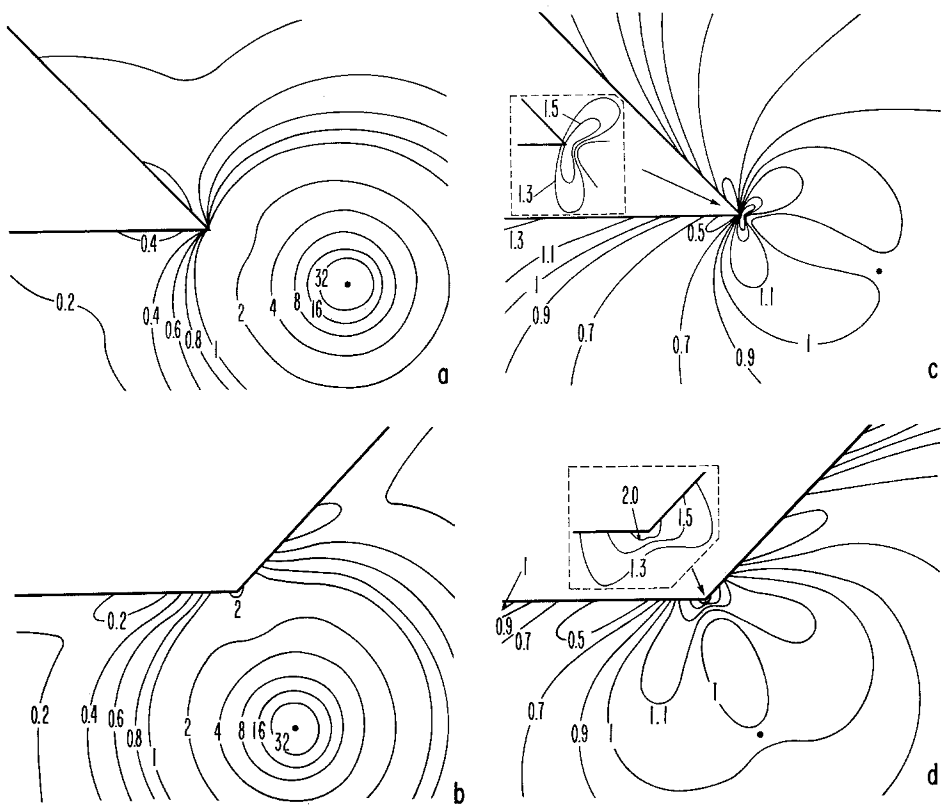

Figure 3 Contour plots of τ and κ, as described for Fig. 2. τ (a) and (b); κ (c) and (d). $\theta_0 = 0$. α: $(7\pi/4)$ in (a) and (c), $5\pi/4$ in (b) and (d). Note that there is no hot spot on the surface.

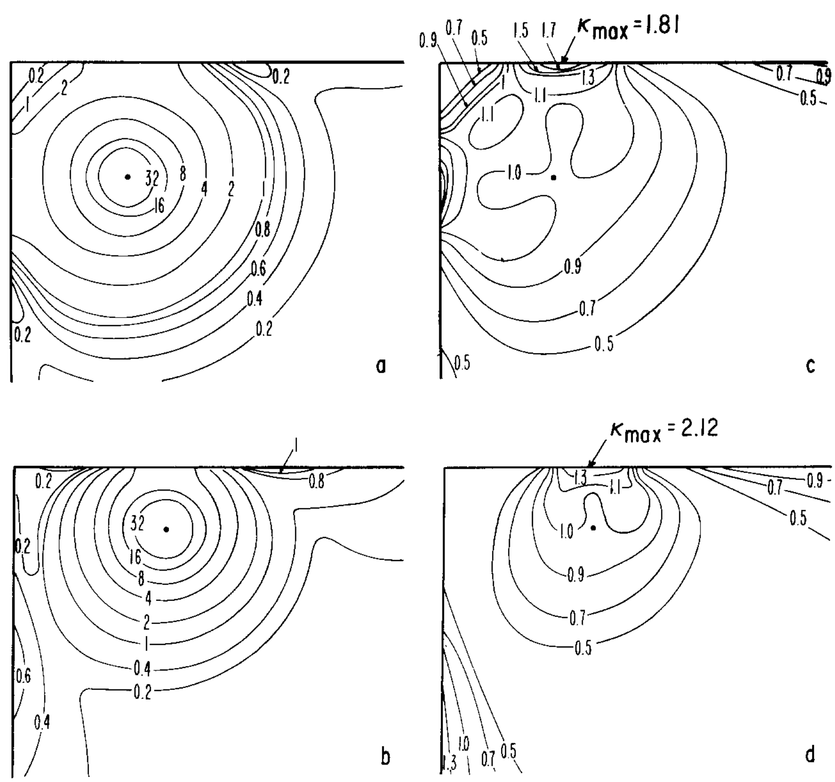

Figure 4 Contour plots of τ and κ, as described for Fig. 2. (a) and (b) τ; (c) and (d) κ, $\alpha = \pi/2$. $\theta_0 = 0$ in (a) and (c), $\pi/8$ in (b) and (d). Note the surface structure in κ, and that κ vanishes at both large and small r.

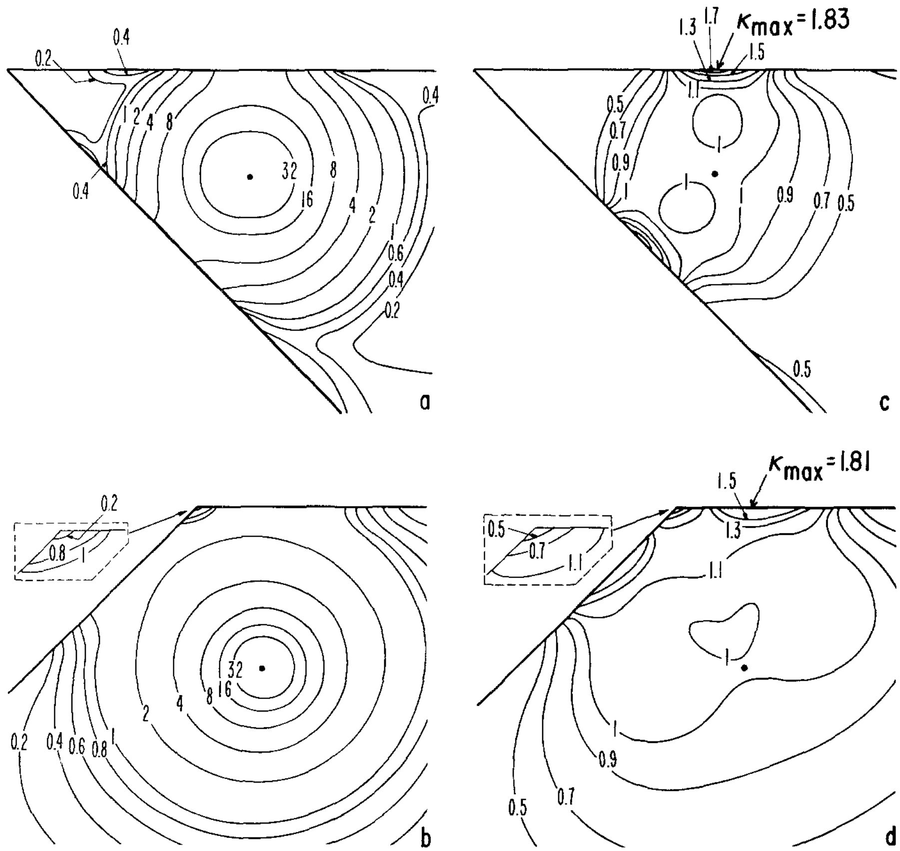

Figure 5 Contour plots of τ and κ, as described for Fig. 2. τ (a) and (b); κ (c) and (d). $\theta_0 = 0$. α: $\pi/4$ in (a) and (c), $3\pi/4$ in (b) and (d).

steps in materials which have been suitably implanted. This surface stress pattern is, of course, strongly dependent on the type of loading, and it is not surprising that the simple surface pressure employed in Marsh's work did not produce it. Experimental test of the results we have found should be straightforward with adaptation of Marsh's photoelastic technique to our form of loading.

In conclusion, we remark that the theoretical machinery we have employed is not limited strictly to point sources of expansion. For example, we have found that a string of misfit dislocations surrounding an inclusion can be modelled by an appropriate array of point sources with about 5% accuracy at distances from the inclusion as small as the misfit spacing [15]. Accordingly, the analysis could be adapted usefully to other stress producing configurations when the comparative simplicity of point sources would be advantageous.

distances large compared to his step-root radius and our source is always a finite distance from a sharp angle vertex.

Initially, the divergence of κ at both large and small r for $\alpha > \pi$ suggested that enhancement might be significant throughout a substantial region near a step root, but that possibility is not confirmed by the numerical results. This implies, for one thing, that stresses due to randomly placed collision cascades, and in particular their nucleation of penny-shaped cracks, cannot be greatly enhanced by surface steps, because of the low geometrical probability of placement in a region of $\kappa > 1$.

The localized regions of significant stress enhancement on the sample surface are interesting. Since it is common for chemical attack to concentrate at points of local stress elevation, we may expect corrosive chemisorption to be accelerated on the top surface as well as at the root of surface

Acknowledgements

We are glad to acknowledge useful conversations with B.O. Hall, F.R.N. Nabarro, and H. Wiedersich. This work was performed under the auspices of the U.S. Energy Research and Development Administration.

References

1. H. NEUBER, "Theory of Notch Stresses: Principles for Exact Calculation of Strength with Reference to Structural Form and Material", 2nd Edn. (Springer, Berlin, 1958) Ch. I and II.
2. N. THOMPSON and N. J. WADSWORTH, *Adv. Phys.* **7** (1958) 72.
3. M. KAMINSKY, J. PEAVEY and S. K. DAS, *Phys. Rev. Letters* **32** (1974) 599; M. KAMINSKY and S. K. DAS, *J. Nucl. Mater.* **53** (1974) 162.
4. M. GUINAN, *ibid.*, 53 (1974) 171.
5. J. E. ROBINSON, B. S. YARLAGADDA and R. A. SACKS, *J. Nucl. Mater.* **63** (1976) 432.
6. P. C. PARIS and G. C. SIH, in "Fracture Toughness Testing and Its Applications" (American Society for Testing and Materials, Philadelphia, 1965) pp. 30-83.
7. D. M. MARSH, in "Fracture of Solids", edited by D. C. Drucker and J. J. Gilman (Interscience, New York, 1962) pp. 119-142.
8. L. D. LANDAU and E. M. LIFSHITZ, "Theory of Elasticity" (Pergamon Press, Oxford, 1959) Ch. 1.
9. J. P. HIRTH and J. LOTHE, "Theory of Dislocations" (McGraw-Hill, New York, 1968).
10. I. N. SNEDDON, "Fourier Transforms" (McGraw-Hill, New York, 1951) pp. 439-444.
11. A. ERDELYI, "Bateman Manuscript Project, Vol. 1, Tables of Integral Transforms", Ed., (McGraw-Hill, New York, 1954).
12. A. H. ZEMANIAN, "Generalized Integral Transforms" (Wiley, New York, 1968) Ch. 4.
13. L. W. WIGGLESWORTH, *Mathematika* **4**, (1957) 76.
14. I. N. SNEDDON and M. LOWENGRUB, "Crack Problems in Classical Theory of Elasticity" (Wiley, New York, 1969) p. 31.
15. R. A. SACKS and J. E. ROBINSON, *Bull. Am. Phys. Soc.* **21** (1976) 1289.

Received 31 August and accepted 4 October 1976.